Sahle, C.J.; Sternemann, C.; Sternemann, H.; Tse, J.S.; Gordon, R.A.;
Desgreniers, S.; Maekawa, S.; Yamanaka, S.; Lehmkuehler, F.;
Wieland, D.C.F.; Mende, K.; Huotari, S.; Tolan, M.:

The Ba 4d-4f giant dipole resonance in complex Ba/Si compounds

In: Journal of Physics B (2014) IOP

DOI: 10.1088/0953-4075/47/4/045102

The Ba 4d–4f giant dipole resonance in complex Ba/Si compounds

Ch.J. Sahle,[1,2] C. Sternemann,[1] H. Sternemann,[1] J.S. Tse,[3] R.A. Gordon,[4] S. Desgreniers,[5] S. Maekawa,[6] S. Yamanaka,[6] F. Lehmkühler,[1,*] D.C.F. Wieland,[1,] K. Mende,[1] S. Huotari,[2,7] and M. Tolan[1]**

[1]Fakultät Physik/DELTA, Technische Universität Dortmund, Dortmund, Germany. Maria-Göppert-Mayer-Str. 2, D-44221 Dortmund, Germany.
[2]Department of Physics, POB 64, FI-00014, University of Helsinki, Helsinki, Finland
[3]Department of Physics and Engineering Physics, University of Saskatchewan, Saskatoon, Canada.
[4]PNCSRF, APS Sector 20, 9700 S. Cass Ave. 435E, Argonne, IL 60439 USA
[5]Department of Physics, University of Ottawa, Ontario, Canada.
[6]Department of Applied Chemistry, Graduate School of Engineering, Hiroshima University, Higashi-Hiroshima 739-8527, Japan.
[7]European Synchrotron Radiation Facility, Boîte Postale 220, F-38043 Grenoble Cedex, France.

E-mail: christian.sternemann@tu-dortmund.de

Abstract. The shape of the Ba 4d – 4f giant dipole resonance is studied for Ba atoms embedded inside complex Si networks covering structures consisting of Si nanocages and nanotubes, i.e. the clathrate Ba_8Si_{46}, the complex compound $BaSi_6$, and the semiconducting $BaSi_2$. Here, non–resonant x–ray Raman scattering is used to investigate **confinement effects on the shape of** the giant resonance in the vicinity of the Ba $N_{IV,V}$–edge. The distinct momentum transfer dependence of the spectra is analyzed and discussed. The measurements are confronted with calculations of the giant resonance within time-dependent local density approximation in the dipole limit. No modulation of the giant resonance's shape for **Ba atoms confined in** different local environments was observed, unlike predicted by **the calculations**. The absence of such shape modulation for complex Ba/Si compounds is discussed providing important implications for further studies of giant resonance phenomena utilizing both theory and experiment.

PACS numbers: 78.70.CK, 71.15.Mb, 82.75.-z

1. Introduction

Giant resonances are intriguing phenomena that have concerned scientists in nuclear,[1] atomic, and condensed matter physics[2] over the past 60 years. These collective excitations can be observed as universal features in nuclei, atoms, clusters, and solids. Although giant dipole resonances (GRs) in atoms and condensed matter have been studied intensively,[3, 4, 5, 6] they have attracted a renewed interest in recent years.[7, 8, 9, 10, 11, 12, 13] Owing to the availability of highly intense synchrotron radiation and advanced experimental setups, new materials can be studied in which resonating atoms are embedded into fascinating complex environments like endohedral fullerenes or silicon based clathrates.

In the early 1990's **theoretical studies proposed that modulations in the fine structure of the GR's shape can be induced if a resonating atom is placed inside complex surroundings as e.g. cage-like nanostructures.[14, 15] Such modulations of the atomic cross section referred to as confinement resonances[16]** depend on the symmetry of the surrounding and the position of the intercalated atom within the nanostructure. This was emphasized by Luberek and Wendin,[17] who presented calculations of the x–ray absorption near–edge spectra of **differently confined Ba in** endohedral fullerenes Ba@C_n. Their calculated spectra show fingerprint–like structures in the shape of the Ba giant dipole resonance in the 4d–4f transition regime depending on the size and the shape of the carbon cages as well as on the position of the guest atom in the cage. Moreover, recently a strong distortion/modulation of the Xe 4d–f GR in Xe@C_{60} was predicted.[18, 19, 20] A comprehensive overview can be found in Ref. [21].

Experimentally, variations in the GR's shape in La– and Ce–halides have been found when compared with the GR in La and Ce metals.[5] Thirty years later, Mitsuke *et al.*[13] observed first experimental evidence for a GR of an atom trapped inside a highly symmetric cage-like environment for ionized Ce@C_{82}. This experiment indicated the existence of **a confinement** resonance but hardly allowed conclusions on its particular shape and fine structure. They extended their studies later to vapors of Dy@C_{82} and Pr@C_{82} and claimed the first hints of GR modulations.[22, 23] Only recently, high quality photoionization spectra of Ce@C_{82}^+ were reported by Müller *et al.*[24] and seemed to exclude the appearance of a GR modulation. However, the detailed analysis of their spectra pointed towards a significant redistribution of decay probabilities of Ce embedded into a carbon cage compared to that of the free atom.[11] In contrast, Kilcoyne *et al.*[9] reported an enhancement of double photo ionization for Xe atoms encaged in C_{60} and in addition found an oscillatory structure in the photo–absorption cross section which they attributed to the multipath interference of the outgoing 4d photo electron wave. **Indeed their findings showed reasonable agreement with calculations concerning oscillatory cross section by analysis in the Fourier reciprocal space.[8]** Despite the extensive search for modulations of the GR **by confinement effects** as predicted by Luberek and Wendin,[17] experimental

evidence of such modulations remains controversial. It was pointed out by Korol *et al.*[25] that the displacement of the resonating atom within the cage due to either a static displacement, i.e. through hybridization with the cage atoms, or thermal excitation can strongly suppress confinement resonances, explaining the discrepancy between theoretical predictions and experimental results. **Recently, calculations of the GR in Ce@C_{82} confirmed the abscence of a confinement resonance in photoionization measurements due to the off-center position of the Ce atom inside the cage.[7]** Lately, the effect of localized bound core-hole excitonic and more delocalized virtual-bound excitonic states on the GR shape was discussed, which should give rise to distinct momentum transfer dependence of the GR spectra.[26]

In this paper, we apply non–resonant x–ray Raman scattering (XRS) as a bulk sensitive probe for the investigation of the corresponding GRs in the vicinity of the Ba $N_{IV,V}$–edges. The experimental data is compared to spectra of the ionic compound $BaSO_4$ and first principles calculations. We present giant dipole resonance spectra of different Ba/Si compounds, in which the Ba atoms are encapsulated in Si structures consisting of Si nano cages and nano tunnels, but observe no significant variations of the **GR for differently confined Ba atoms unlike predicted by our calculations**. We discuss the origin of the GR modulations and give suggestions for further studies of GR phenomena using theoretical and experimental approaches.

2. Experimental

Ba/Si systems can be synthesized in a manifold of crystalline structures so that resonating Ba atoms can be investigated when embedded in a variety of highly symmetric Si environments.[27] More precisely, we study the Si clathrate Ba_8Si_{46}, in which the Ba atoms are placed in two different types of Si nano cages, as well as the compounds $BaSi_6$, $BaSi_2$, and $BaSO_4$.

Ba_8Si_{46} has two non-equivalent Ba atoms in each unit cell: one of which occupies a Si_{20} and one a Si_{24} cage. Two pentagonal dodecahedra (Si_{20}) and six tetrakaidecahedra (Si_{24}) are connected by sharing faces forming a space filling crystal structure with space group $Pm\bar{3}n$.[28] Part of the Si nano-cages in Ba_8Si_{46} form tube–like structures. $BaSi_6$ (space group Cmcm) is built up of irregularly shaped Si_{18} polyhedra containing one Ba atom.[27] These polyhedra are connected by sharing faces and thus form Si nanotubes containing chains of Ba atoms. The structures of the different Ba containing clathrates and compounds under investigation are shown in Fig. 1 together with the local environment of the non-equivalent atoms in the respective unit cell.

The Ba GR in a solid has been studied for metallic Ba,[30] Ba halides,[31, 32] $YBa_2Cu_3O_{7+x}$,[33] Ba_8Si_{46},[12] and $BaSO_4$ [34] but without a systematic investigation of possible shape modulations. Because the Ba–doped Si clathrate and $BaSi_6$ have structures comparable to the Ba@C_n network, for which Luberek and Wendin[17] predicted strong confinement resonances, the spectra of the Ba GR are expected to be sensitive to the particular surrounding of the Ba atoms. Hence, these compounds

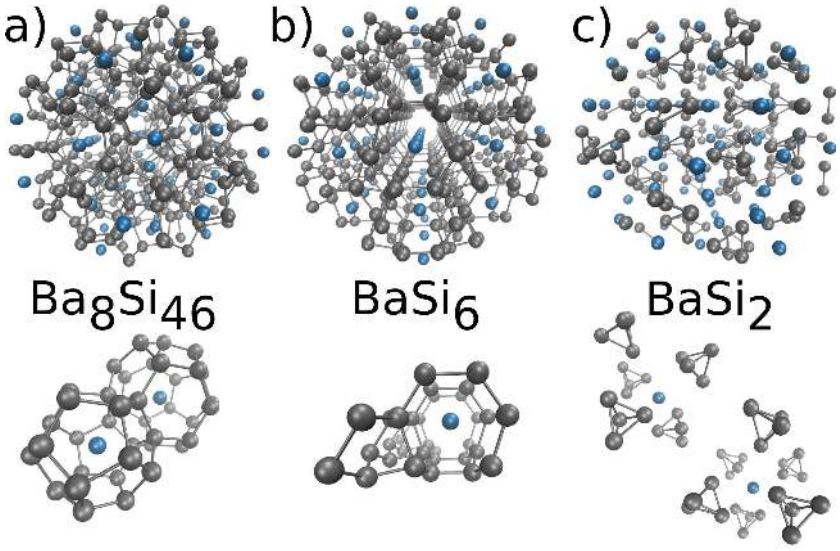

Figure 1. Visualization of the different complex Si–based compounds: a) Ba_8Si_{46}, b) $BaSi_6$, and c) $BaSi_2$ (top). Stick and ball sketches of the immediate surroundings of the two different unique Ba atoms in the two different cages for Ba_8Si_{46}, the single unique Ba atom in an Si nano-tube/tunnel for $BaSi_6$, and the two different unique Ba atoms of $BaSi_2$ (bottom).

are valuable systems in order to study modifications of the Ba GR in detail.

Non–resonant x–ray Raman scattering (often also referred to as non–resonant inelastic x–ray scattering (NRIXS or NIXS))[35] has been used here to study the GR of the different Ba/Si compounds. This energy loss technique allows one to investigate shallow absorption edges using high energy x–rays yielding high bulk sensitivity, and even to use it as a contrast mechanism for 3D imaging in bulk scale.[36] The measured quantity in an XRS experiment is the double differential scattering cross section $(\mathrm{d}^2\sigma/\mathrm{d}\Omega\mathrm{d}\omega)$, which is related to the dynamic structure factor $S(\mathbf{q},\omega)$ by

$$\frac{\mathrm{d}^2\sigma}{\mathrm{d}\Omega\mathrm{d}\omega} = \left(\frac{\mathrm{d}\sigma}{\mathrm{d}\Omega}\right)_{\mathrm{Th}} \frac{\omega_2}{\omega_1} S(\mathbf{q},\omega). \tag{1}$$

Here, $\left(\frac{\mathrm{d}\sigma}{\mathrm{d}\Omega}\right)_{\mathrm{Th}}$ is Thomson's scattering cross section, $\hbar\omega_1$ and $\hbar\omega_2$ are the incident and scattered photon energies with the energy transfer $\hbar\omega = \hbar\omega_1 - \hbar\omega_2$ and momentum transfer $\mathbf{q}$. The dynamic structure factor can be expressed via

$$S(\mathbf{q},\omega) = \sum_{\mathrm{f}} \left|\langle \mathrm{f}|e^{i\mathbf{q}\cdot\mathbf{r}}|\mathrm{c}\rangle\right|^2 \delta(E_\mathrm{c} - E_\mathrm{f} + \hbar\omega), \tag{2}$$

which describes an excitation from a core state $|\mathrm{c}\rangle$ with energy E_c to **both unoccupied bound and continuum** states $|\mathrm{f}\rangle$ with energy E_f. The operator $e^{i\mathbf{q}\cdot\mathbf{r}}$ gives rise to the $\mathbf{q}$-dependence of the scattering cross section opening non-dipole excitation channels with increasing $|\mathbf{q}|$. According to this, $\hbar\omega$ can be tuned in the vicinity of soft x–ray

absorption edges by variation of the incident energy at fixed analyzer energy and the momentum transfer **q** can be changed via the scattering angle. The absolute value of $q = |\mathbf{q}|$ determines the contribution of dipole and multipole transitions to the scattering spectrum. In the low-q (dipole) limit, the information obtained by an XRS experiment is similar to that of soft x-ray absorption spectroscopy. **As long as $qa \ll 1$, with the electron orbital radius a, dipole excitations dominate the excitation spectrum, i.e for Ba 4d electrons $q < 1.25\text{Å}^{-1}$ with $a = 0.8\text{Å}$.** At higher momentum transfers, XRS becomes sensitive to **non-dipole allowed transitions[37] and/or high order multiplet features, e.g., in the 3d transition metals, 4f rare earth elements, and 5d actinides.[26, 41]. Such transitions dominate the XRS spectra in case of the Ba compounds studied here for $q > 6\text{Å}^{-1}$ as can be estimated from the transition matrix elements discussed later. This XRS spectroscopy is a well established probe of the local atomic and electronic structure particularily when high bulk sensitivtiy is required.**

Ba_8Si_{46} and $BaSi_6$ powder samples were prepared under high–temperature and high–pressure conditions as described in Refs. [29, 28, 27]. As a reference to extract the pure Ba contribution from the XRS spectra of the different Ba/Si compounds, powders of polycrystalline Si and the empty clathrate Si_{136} were also measured. The empty Si_{46} clathrate, which would be the adequate reference sample for Ba_8Si_{46}, cannot be synthesized. The quality of all samples was confirmed by x–ray diffraction. A first experiment (run 1) was performed utilizing the multiple–analyzer–crystal spectrometer for non–resonant inelastic x–ray scattering spectroscopy at the European Synchrotron Radiation Facility (ESRF) beamline ID16. A detailed description of the instrument can be found elsewhere.[38] At an analyzer energy of 9.687 keV, bent Si(660) single crystals located on a 1–m diameter Rowland circle focus the analyzed x–rays onto a Maxipix pixel detector. In this way, XRS spectra for three different momentum transfers $q = 1.90$, 2.51, and 3.11 Å^{-1} were recorded simultaneously. Employing the Si(111) monochromator together with a Si(220) channel cut monochromator, a total energy resolution of 1.1 eV was obtained. The samples were kept under vacuum conditions during the XRS measurements. In a second experiment (run 2) a Ba_8Si_{46} powder sample was measured employing the LERIX setup[39] at the undulator beamline 20ID–B of sector 20 of the Advanced Photon Source (APS). Using the Si(111) double crystal monochromator and the Si(444) analyzer reflection at fixed analyzer energy of 7.9 keV an overall energy resolution of 0.9 eV was achieved. Scattering angles between 9-171° allowed to record momentum transfer values between 1.27-8.10 Å^{-1}. The Ba_8Si_{46} sample was kept in a He flushed chamber during the measurement.

The acquired spectra were corrected for the Thomson scattering cross section, absorption, and background. The signal of the Ba atoms has to be extracted from the underlying spectral contribution of the Si atoms, i.e. the Si valence electron spectrum together with the Si core electron contribution at the Si $L_{II,III}$–edge. This was done by subtraction of the Si reference spectrum from the data. Alternatively, the Si_{136} reference spectrum was used, but no significant change of the resulting spectra was found. Finally,

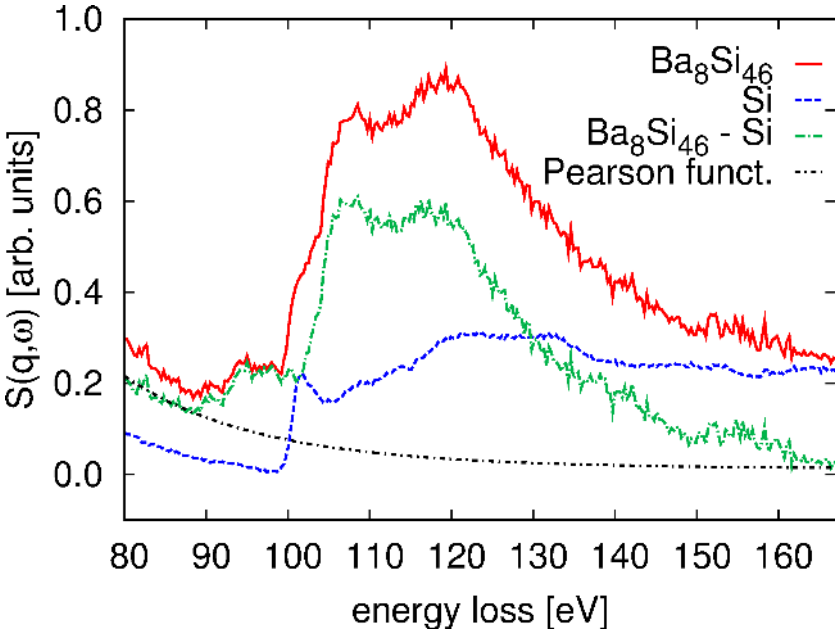

Figure 2. Extraction of the Ba GR for Ba_8Si_{46} at $q = 2.63$ Å^{-1}. The Si contribution is removed from the raw data (solid line) by subtraction of the underlying Si spectrum (dashed line) measured at the same q. Finally, the decreasing tail of the valence electron contribution of the resulting Ba spectrum (long dashed-dotted line) is approximated by a Pearson VII function (short dashed-dotted line) and can be subtracted accordingly.

the pure Ba $N_{IV,V}$–XRS spectrum with the Ba 4d–f giant resonance was obtained by subtraction of the high energy–loss tail of the Ba valence–electron contribution, which was modeled using parameterized Pearson VII functions, and was normalized to the area between 101 eV and 150 eV energy loss. An example of a typical extraction procedure is presented in Fig. 2 for Ba_8Si_{46} measured at $q = 2.63$ Å^{-1}. A thorough description of the data analysis of XRS spectra is given in Ref. [40].

3. Results and discussion

The extracted XRS spectra of the Ba 4d–f GRs for run 1 are shown in Fig. 3 a) for the different Ba/Si compounds for the lowest momentum transfer of $q = 1.90$ Å^{-1} together with the result of the ionic compound $BaSO_4$ taken from Ref. [34]. The pre–edge features between 90–101 eV energy loss, most prominently observed for $BaSO_4$, are predominantly due to non dipole allowed multiplet transitions and thus gain significant spectral weight for large momentum transfers. These multiplet–like features, which are sensitive to hybridization, e.g., under high pressure, have recently been used to study hybridization in the ionic compounds $CePO_4$ and $LaPO_4$[41] and pressure induced electronic topological phase transitions in Ba_8Si_{46}.[42]

The GR itself dominates the XRS spectra for energy losses between 101 and 165 eV. In this energy range, all materials show a two peak structure with two

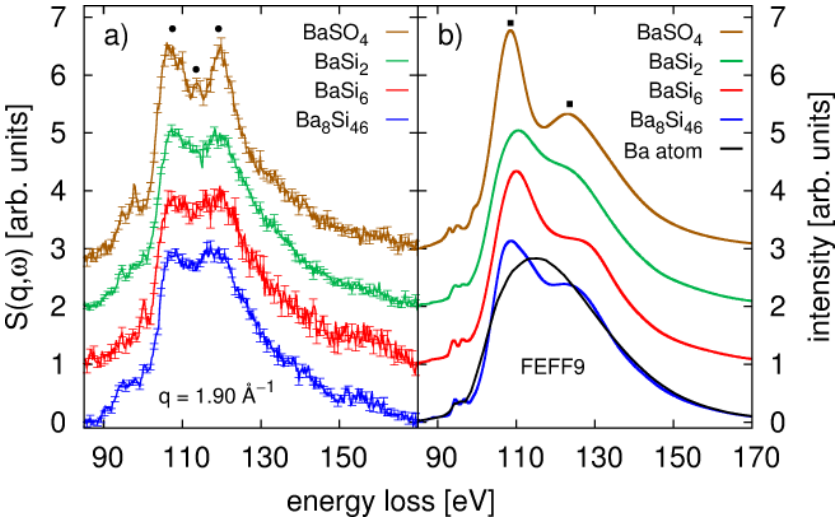

Figure 3. a) Extracted XRS spectra of the Ba 4d–f GR in the vicinity of the Ba $N_{IV,V}$ –edge for the different compounds measured at $q = 1.90$ Å^{-1}. The spectra are vertically shifted for clarity. b) RSMS calculations of the **Ba GR in the different compounds and in atomic Ba** using the TDLDA exchange kernel in FEFF9.

broad features at 107.5 and 119 eV and most prominent a minimum/shoulder in between the two peaks. Whereas the spectra of $BaSi_2$, $BaSi_6$, and Ba_8Si_{46} are very similar, the GR of $BaSO_4$ exhibits two pronounced maxima at 107.5 and 119 eV and another small peak at 112.5 eV within the dip between the maxima (see small black dots in Fig. 3). Similar characteristic features of ionic compounds have been observed earlier for BaF_2 [32] and $BaCl_2$ [31]. The GRs of the different Ba containing compounds were modeled using the real–space multiple–scattering (RSMS) approach FEFF[43] within the time–dependent local density approximation (TDLDA) to account for collective phenomena. Such a comparison with experiments is justified only for very small momentum transfers when multipole excitations play a minor role (see e.g. Refs. [12, 34, 44] for details). To simulate the spectra of the investigated compounds, the Ba $N_{IV,V}$ absorption edge spectra were calculated for each non–equivalent atom in the unit cell and the resulting spectra were added up accounting for the corresponding multiplicities. **For comparision we calculated also the spectrum of atomic Ba. In all cases, dynamic screening was used in the TDLDA calculations.[43]. The calculations, except for atomic Ba, were converged with respect to the size of the real space clusters. Typically, convergence was achieved using approx. 60 atoms in the self consistent iteration of the atomic potentials and a cluster of approx. 100 atoms for the full multiple scattering calculation. We used the Hedin-Lundquist exchange and correlation potential for all calculations. Spectra of N_{IV} and N_V edges were calculated separately and added. The resulting sum spectra of the Ba $N_{IV,V}$ edge were shifted on the energy scale to coincide with the experimental data at the onset of the GR. All simulated spectra were convoluted with a Gaussian function of 1**

eV width to account for the experimental energy resolution. The results of the calculations are presented in Fig. 3 b). **Apparently, the confinement effect on the GR can be directly seen when the spectra of encapsulated Ba atoms are compared to that of atomic Ba and manifests in an oscillatory shape of the GR which is also found in the experiment when the first maximum in the GR is considered. The profile of the measured confinement resonances is well reproduced by theory and a qualitative agreement can be observed.** However, the second maximum around 119 eV is strongly suppressed in the calculated spectra of all materials as compared to the experimental findings. It has been discussed earlier that besides a possible dipole resonance modulation predicted by Wendin[14], double ionization processes[45] might contribute to the spectrum in the energy loss range between 111 and 130 eV[34] and that such double electron excitations can obscure the GR's shape.[4, 46, 11] Double ionization processes are not accounted for in the theoretical approach. Likewise, the finite momentum transfer present in the XRS measurements even at the smallest q values, i.e. non-negligible contributions arising from multipole transitions in the experimental spectra which point toward the existence of different excitation channels, could complicate a direct comparison of the overall GR's shape with theory. Nevertheless, while the simulations of all Ba/Si compounds show a smooth peak/shoulder structure, $BaSO_4$ exhibits two clear maxima in unison with experiment.

In order to investigate the discrepancies between the calculated and experimental results, we will first discuss the full momentum transfer dependence of the XRS spectra, illustrating with Ba_8Si_{46}. Using XRS the GR can be studied only for small momentum transfer as with increasing momentum transfer multipole transitions gain significant spectral weight, strongly suppressing the observed GR intensity. Thus, in both excitation regimes XRS probes very different properties of the material which demand also different theoretical description. In the dipole limit the collective GR phenomenon can be modeled by methods employing time-dependent local density approximation whereas in the multipole limit local atomic excitations can be described by momentum transfer dependent atomic multiplet calculations. Extracted spectra of Ba_8Si_{46} measured over a larger momentum transfer range are depicted in Fig. 4. A direct comparison between spectra of run 1 and run 2 averaged over momentum transfers between 1.90–3.17 $Å^{-1}$ is shown in Fig. 4 a) and demonstrates the accordance of the two experimental data sets. The higher statistical accuracy of data obtained from run 1 favors this data set for all detailed discussions except for the momentum transfer dependence. Spectra for each momentum transfer are shown in Fig. 4 b). The second maximum of the GR around 119 eV gains significant spectral weight with increasing momentum transfer. This is quantified by the ratio of the height of the second and first peak (at 107.5 eV), which is plotted against the corresponding momentum transfer in Fig. 4 c). Linear regression of the data points in Fig. 4 c) and extrapolation to $q = 0$ closely resembles the peak height ratio of the TDLDA calculation for Ba_8Si_{46}. Thus, contributions arising from a finite momentum transfer in the experimental spectra largely account for the difference in spectral weight in the

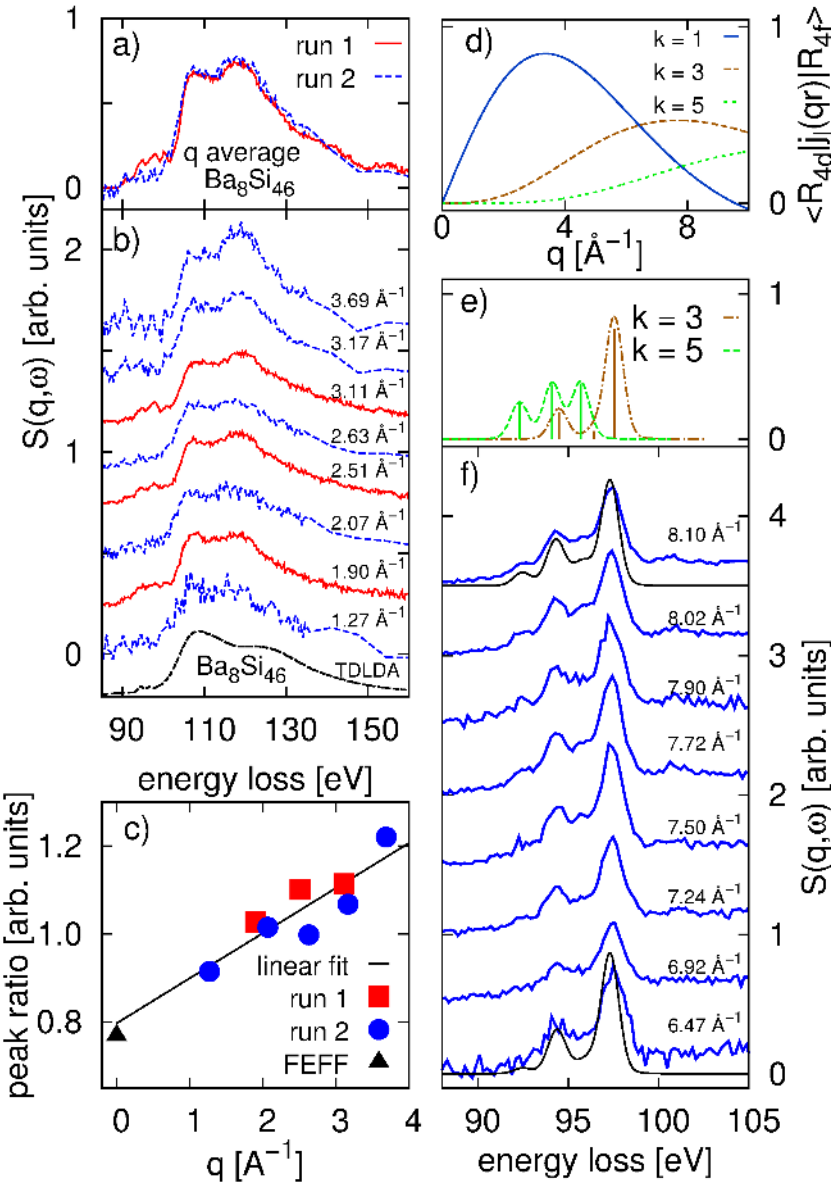

Figure 4. a) Comparison of averaged spectra of $Ba_{24}Si_{100}$ from run 1 and run 2 (see text for details). b) q-dependence of the GR in Ba_8Si_{46} for momentum transfers between 1.27 and 3.69 Å^{-1}. Throughout the figure, solid lines correspond to run 1, dashed lines to run 2. c) Peak height ratios as discussed in the text for Ba_8Si_{46} plotted against the according momentum transfer and extrapolation to $q = 0$ together with the peak hight ratio determined from the FEFF simulation. **d) Calculated matrix elements for k = 1 (dipole), 3 (octupole), and 5 (triakontadipole) transitions from atomic multiplet calculations of Ba^{2+}. e) Stick- and broadened spectra of the octupole (k = 3) and triakontadipole (k = 5) transitions from atomic multiplet calculations.** f) Experimental high-q spectra of Ba_8Si_{46} for q-values between 6.47 and 8.10 Å^{-1} together with calculated spectra for the lowest and highest momentum transfers shown.

vicinity of the second maximum of the GR when compared with theory. Thus one can conclude that it is the momentum transfer dependence of the GR XRS spectra which causes the strong differences between theory and experiment for energy losses around 119 eV, whereas spectral signatures due to double electron ionization can be assumed to have only minor effect on the spectral shape of the GR. The momentum transfer dependence of the spectra might point toward an additional contribution to the GR which is strengthened at higher momentum transfer (i.e. increase of the feature at 119 eV). Such a contribution possibly arises from virtual bound states having more localized character and thus increase in intensity with increasing momentum transfer, much like a multiplet feature.[26] For even higher momentum **transfers, the high order multipole transitions become dominant over the dipole allowed GR at low momentum transfer as can be seen from the calculated transition matrix elements (see Fig. 4 d)).** These high order multiplet features can readily be understood in terms of atomic multiplet theory [47], which reproduces all spectral features (see Fig. 4 e) and f)) including the q-dependence at high momentum transfers (note that the shown spectra at these high momentum transfers were not corrected for the signal of the underlying Si $L_{II,III}$ edges). For the comparison of the calculated multiplet spectra with experiment, the calculated stick spectra were convoluted with a Lorentzian of width 0.1 eV to account for the finite core hole lifetime and a Gaussian of width 0.9 eV to account for the experimental energy resolution. Slightly smeared multiplet features, as seen here in comparison to the calculated spectra from the atomic multiplet theory, were found before for Ba_8Si_{46} and stem from the hybridized nature of the guest-host interaction. [42]

We conclude that for a study of the Ba GR using XRS the measurements have to be restricted to momentum transfers less than 4 $Å^{-1}$ to obtain significant GR intensity with only small contribution of multipole excitations. Furthermore, for an unambiguous interpretation of the spectra, in principle a TDLDA scheme that considers the momentum transfer dependence of XRS would be required. For a full understanding of the experimental spectra over the entire q-range measured, a unified theoretical approach, such as suggested recently in Ref. [26], is highly desirable. Here, especially the exact nature of the q-dependence of the GR is interesting and would allow for a comprehensive comparison between experiment and theory providing a detailed analysis of confinement effects.

It is now worthwhile to discuss the GRs in more detail in terms of confinement resonances. In Ba_8Si_{46} and $BaSi_6$, the Ba atoms are embedded in connatural Si environments differing most prominently by the symmetry of the Si host cages. To inspect the influence of confinement on the GR we next only compare the spectra of the Ba/Si systems (Fig. 5 a) for all q-values measured in run 1) by plotting the spectral differences between Ba_8Si_{46} and $BaSi_2$ from that of $BaSi_6$, i.e. by taking $BaSi_6$, which has only equivalent Ba atoms confined in a well defined tunnel-like surrounding, as reference. The differences are plotted in Fig. 5 b) for the three momentum transfers measured in run 1. In this representation, a confinement modulation effect due to

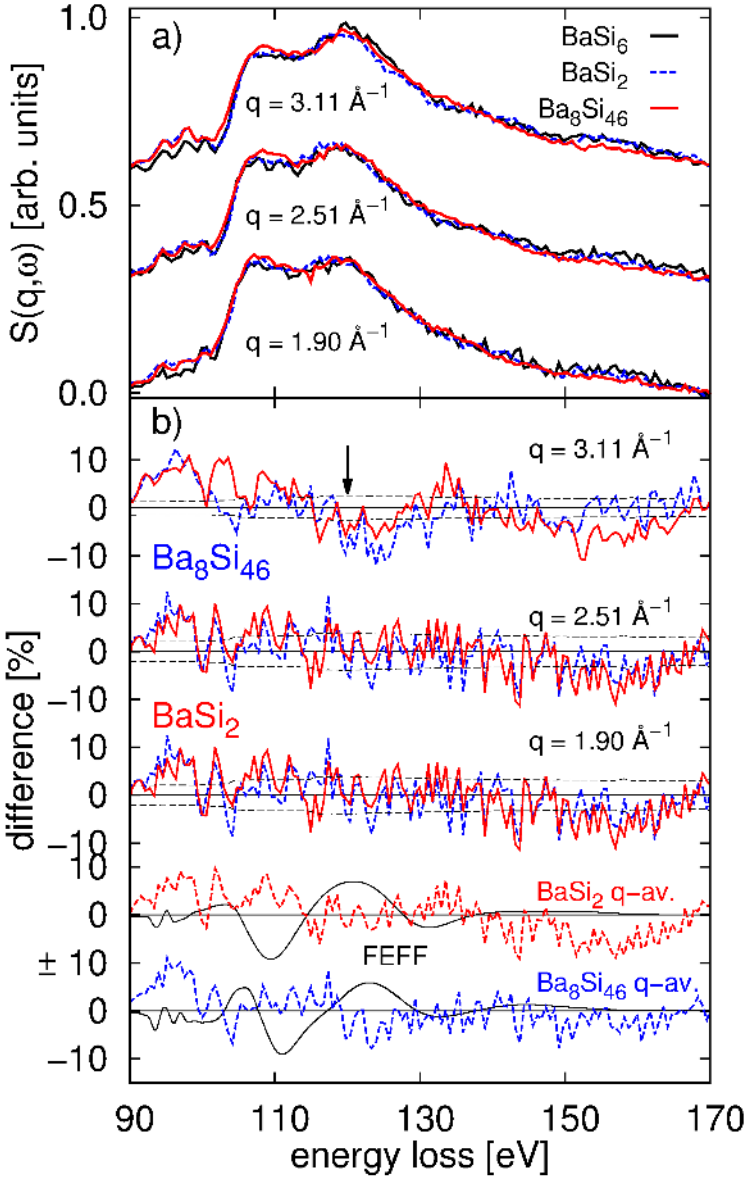

Figure 5. a) Measured spectra of the different Ba/Si compounds for each momentum transfer of run 1 in direct comparison (offset vertically with increasing momentum transfer, two data points binned). b) Calculated differences between Ba_8Si_{46} and $BaSi_6$ (dashed) and $BaSi_2$ and $BaSi_6$ (solid) from a) of the same figure (small dshed lines represent typical 0 of the experimental differences as derived from the counting statistics). The differences are plotted for each of the measured momentum transfers of run 1 and averages over the two smallest q-values of the above differences are compared to differences of the according the TDLDA calculations (solid lines).

different Ba environments would be visible as a dissimilar differences between Ba_8Si_{46} and $BaSi_6$ (dashed curves) on the one hand and $BaSi_2$ and $BaSi_6$ (solid curves) on the other. Such deviations in the spectral region of the GR (101–165 eV energy loss) are hardly observed for any of the momentum transfers. Moreover, the momentum transfer dependence of the differences is small with slight changes in the differences taken at q= 3.11 $Å^{-1}$, which can be related to changes in the vicinity of the second peak of the GR spectra of the different compounds (see arrow). Thus, for a comparison with theory we use an average over the differences obtained for the two lowest momentum transfers. These *q*-averaged differences for both compounds are plotted at the bottom of the figure and are compared to the differences calculated from the simulated GR data. It is notable that the results of experiment and theory are in strong disagreement.

We infer that the predicted spectral changes of the GR cannot be confirmed by experiment. In the following we will discuss the shape of the calculated spectra in more detail for the non-equivalent Ba positions and give possible reasons, beside a remaining momentum transfer dependence, for the discrepancy between theoretically predicted confinement modulations and our experimental findings, i.e. the deviation of the surroundings of the embedded Ba atom from a highly symmetric environment and the effect of off-center position of the Ba atom.

The influence of the direct environment on the shape of the GR is best seen when the simulated spectra are decomposed to the contributions from all unique atoms as is shown in Fig. 6. Apart from the ionic $BaSO_4$, Ba atoms in cage like surroundings (such as both unique Ba atoms in Ba_8Si_{46} and the one Ba atom in $BaSi_6$) show a pronounced bimodal GR, whereas in $BaSi_2$ the GR is smeared out to a peak/shoulder structure. In particular, the shape of the GR spectra from the two different Ba atoms in Ba_8Si_{46} directly reflect the confinement effect, as the position of the second maximum is at higher energies for the $Ba_{(0)}$ atom, which is contained in the smaller cage (Si_{20}), compared to $Ba_{(1)}$ which is contained in the larger cage (Si_{24}). Obviously, in an experiment these two confinement effects are averaged over, which will smear out their distinct features. **It was shown earlier that confinement resonances are expected to be suppressed if the endohedrally encaged atom is displaced from the cage center.[7, 25]** To investigate possible effects of a distortion of the cage or an off-center position of the intercalated Ba atom, we modeled the GR resonance from a Si_{24}-cage by successively reducing the number of Si atoms of the cage and successively increasing the off-center position of a Ba atom, respectively. Thus, in both series of calculations an increasing degree of artificial asymmetry is induced to observe systematic changes in the resulting spectra. **The details of the calculations have been already discussed** and the results are shown in Fig. 7 a) and b). Opening up a Si_{24} cage, i.e. breaking the symmetry of the cage, shifts the first maximum to slightly higher energy losses and most notably reduces the intensity of the second maximum. The characteristic minimum is smeared out. A similar trend can be observed when the Ba atom is displaced from the center of the cage,[42] i.e. the first maximum shifts to higher energy losses and the two peak structure disappears. **This is in line with the results of Refs. [7, 25].** All these

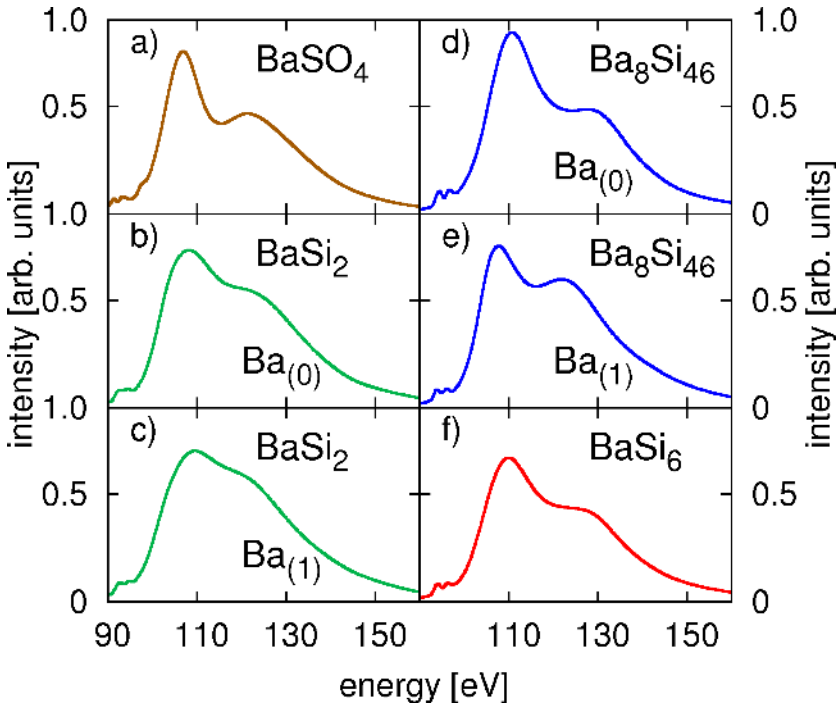

Figure 6. Calculated Ba GR spectra for the non–equivalent Ba atoms of the different compounds: a) Spectrum from the only unique Ba atom in $BaSO_4$; b) - c) calculated spectra of the two unique Ba atoms of $BaSi_2$. d) - e) Spectra from the two different unique Ba atoms of Ba_8Si_{46} (one contained in a Si_{20} (d) and one contained in a Si_{24} cage (e)). f) Calculated spectrum from the Ba atom in the tunnel–forming Si_{18} cages of $BaSi_6$.

effects can obscure the modulation of the GR's shape due to a specific environment of the embedded Ba atom in the different Ba/Si compounds and hinder a straightforward and unambiguous interpretation of the spectra.

4. Summary and conclusion

We investigated the shape of the Ba 4d – f giant dipole resonance of Ba atoms embedded inside the complex Si networks Ba_8Si_{46}, $BaSi_6$, and $BaSi_2$. Experimental results do not exhibit any pronounced variation **in the Ba $N_{4,5}$ confinement resonances for the different local environments. This is in contrast to theoretical predictions based on FEFF using TDLDA, which may be related to breaking the symmetry of the Ba atom with respect to its surrounding.**

For a thorough investigation of such modulations it is necessary to study atoms embedded in highly symmetric environments such as fullerenes, which have only equivalent positions of the embedded atom. An inducible change in the local environment of the encapsulated atom, using e.g. temperature or pressure, to produce a deviation from high-symmetry, would allow to directly tracking changes in the shape of confinement resonances. Here,

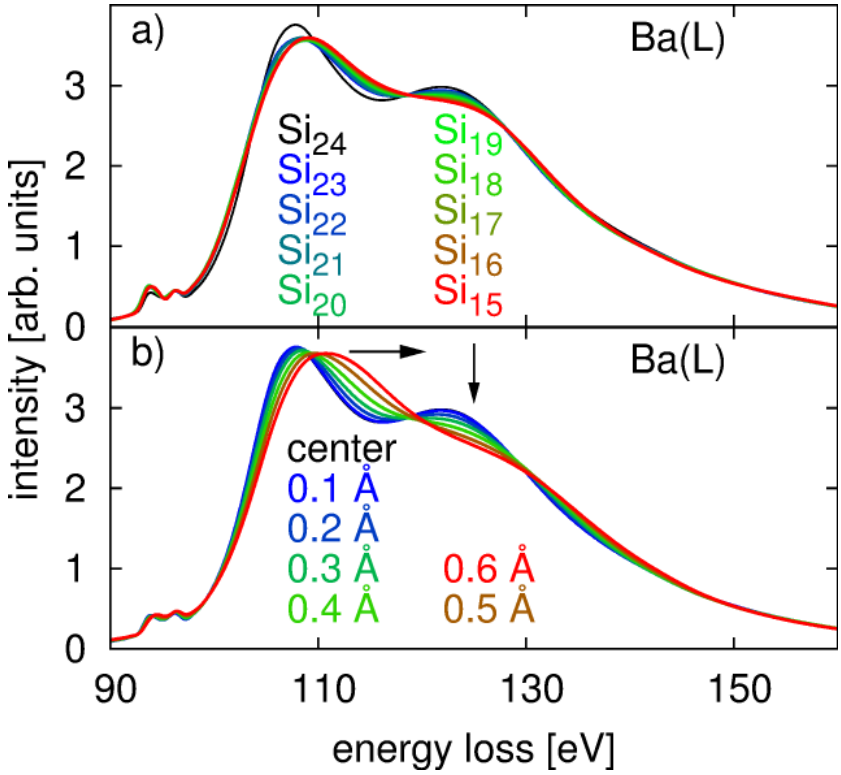

Figure 7. a) Series of calculations of the GR of a Ba atom in a symmetric Si_{24} cage showing the influence of consecutively stripping Si atoms from the cage. With a decreasing number of Si atoms in the cage, the first maximum shifts slightly to higher energy losses whereas the second maximum loses spectral weight. b) Influence of an asymmetric position within a Si_{24} cage by a series of calculations where the Ba atom is consecutively displaced from the center. The first maximum shifts towards higher energies while the second maximum loses intensity. All calculations show a smearing of the spectral features when asymmetry is induced.

XRS will be a valuable technique allowing for bulk sensitive GR studies in complex sample environments such as high temperature and pressure cells, not feasible with other methods.

After submission of this article Phaneuf et al.[48] published an experimental and theoretical study of confinement resonances of photoionized Xe encaged in C_{60}^{+}. They found unprecedented evidence of redistribution of oscillator strength due to multipath interference of the excited photoelectron. Their observation of a GR modulation by embedding an atom into a highly symmetric environment when compared to the atomic cross section is in agreement with the particular shape of the GR for less symmetric complex Ba/Si compounds found in our study.

5. Acknowledgments

We would like to acknowledge the ESRF and APS for providing synchrotron radiation and technical support. PNC/XSD facilities at the Advanced Photon Source, and research at these facilities, are supported by the US Department of Energy - Basic Energy Sciences, a Major Resources Support grant from NSERC, the University of Washington, Simon Fraser University, and the Advanced Photon Source. Use of the Advanced Photon Source, an Office of Science User Facility operated for the U.S. Department of Energy (DOE) Office of Science by Argonne National Laboratory, was supported by the U.S. DOE under Contract No. DE-AC02-06CH11357. This work was supported by DFG (Grants Tol169/5-5 and TO 169/14-1), BMBF (Grants 05KS7PE1 and 05K10PEC), DAAD (313-PPP-SF/06-IK/08-IK), the Academy of Finland (Grants 1256211, 1127462, and 1259526), and the University of Helsinki Research Funds (Grants 490076 and 490064). We would like to thank J.A. Soininen for stimulating discussions. H. Jiang is kindly acknowledged for support during TEM/ EELS measurements on Ba_8Si_{46}.

References

* present address: Deutsches Elektronen Synchrotron (DESY), D-22607 Hamburg, Germany
** present address: Helmholtz-Zentrum Geesthacht, D-22607 Hamburg, Germany
[1] Berman B L and Fulz S C 1975 *Revs. Mod. Phys.* **47** 713
[2] Connerade J P, Esteva J M and Karnatak R C (edt.) 1987 *Giant Resonances in Atoms, Molecules, and Solids* (Plenum, New York)
[3] Bréchignac C and Connerade J P 1994 *J. Phys. B: At. Mol. Opt. Phys.* **27** 3795
[4] Richter M, Meyer M, Pahler M, Prescher T, Raven E V, Sonntag B, and Wetzel H E 1989 *Phys. Rev. A* **39** 5666
[5] Suzuki S, Ishii T, and Sagawa T 1975 *J. Phys. Soc. Japan* **38** 156
[6] Wendin G 1973 *Phys. Lett. A* **A–46** 119
[7] Chen Z and Msezane A Z 2013 *Phys. Rev. A* **88** 043423
[8] Patel A B and Chakraborty H S 2011 *J. Phys. B: At. Mol. Opt. Phys.* **44** 191001
[9] Kilcoyne A L D, Aguilar A, Müller A, Schippers S, Cisneros C, Alna'Washi G, Aryal N B, Baral K K, Esteves D A, Thomas C M and Phaneuf R A 2010 *Phys. Rev. Lett.* **105** 213001
[10] McCune M A, Madjet M E and Chakraborty H S 2009 *Phys. Rev. A* **80** 011201
[11] Müller A, Schippers S, Habibi M, Esteves D, Wang J C, Phaneuf R A, Kilcoyne A L D, Aguilar A and Dunsch L 2008 *Phys. Rev. Lett.* **101** 133001
[12] Sternemann H, Sternemann C, Tse J S, Desgreniers S, Cai Y Q, Vankó G, Hiraoka N, Schacht A, Soininen J A and Tolan M 2007 *Phys. Rev. B* **75** 245102
[13] Mitsuke K, Mori T and Kou J 2005 *J. Chem. Phys.* **122** 064304
[14] Wendin G and Wästberg B 1993 *Phys. Rev. B* **48** 14764
[15] Puska M J and Nieminen R M 1993 *Phys. Rev. A* **47** 1181; Puska M J and Nieminen R M 1994 *Phys. Rev. A* **49** 629
[16] Connerade J P, Dolmatov V K and Manson S T 2000 *J. Phys. B: At. Mol. Opt. Phys.* **33** 2279
[17] Luberek J and Wendin G 1996 *Chem. Phys. Lett.* **248** 147
[18] Amusia M Y, Baltenkov A S, Chernysheva L V, Felfi Z and Msezane A Z 2006 *J. Exp. Theor. Phys.* **102** 53
[19] Dolmatov V K and Manson S T 2008 *J. Phys. B: At. Mol. Opt. Phys.* **41** 165001

[20] Madjet M E, Renger T, Hopper D E, McCune M A, Chakraborty H S, Rost J M and Manson S T 2010 *Phys. Rev. A* **81** 013202
[21] Dolmatov V K 2009 *Advances in Quantum Chemistry: Theory of Confined Quantum Systems* edited by J. R. Sabin and E. Brändas (Academic Press, New York) **58** 13
[22] Mitsuke K, Mori T, Kou J, Haruyama Y, Takabayashi Y and Kubozono Y 2005 *Int. J. Mass. Spectrom.* **243** 121
[23] Katayanagi H, Kafle B P, Kou J, Mori T, Mitsuke K, Takabayashi Y, Kuwahara E and Kubozono Y 2008 *J. Quant. Spectrosc. Radiat. Transfer* **109** 1590
[24] Müller A, Schippers S, Phaneuf R A, Habibi M, Esteves D, Wang J C, Kilcoyne A L D, Aguilar A, Yang A and Dunsch L 2007 *J. Phys. Conf. Ser.* **88** 012038
[25] Korol A V and Solov'yov A V 2010 *J. Phys. B: At. Mol. Phys.* **43** 201004
[26] Sen Gupta S, Bradley J A, Haverkort M W, Seidler G T, Tanaka A and Sawatzky G A 2011 *Phys. Rev. B* **84** 075134
[27] Yamanaka S and Maekawa S 2006 *Z. Naturforsch.* **61b** 1493
[28] Yamanaka S, Enishi E, Fukuoka H and Yasukawa M 2000 *Inorg. Chem.* **39** 56
[29] Fukuoka H, Ueno K and Yamanaka S 2000 *J. Organometallic Chem.* **611** 543
[30] Rabe P, Radler K and Wolff H W 1974 *IV international Conference on Vacuum Ultraviolet Radiation Physics Hamburg* in *Vacuum UV Radiation Physics* ed. E. E. Koch *et al.* (Vieweg-Pergamon, Berlin).
[31] Rabe P 1974 *Ph.D. Thesis* (Universität Hamburg,Hamburg)
[32] Hecht M H 1982 *Stanford Synchrotron Radiation Laboratory Report No. 82/07* unpublished. The spectrum of BaF_2 has been published in Ref. [33].
[33] Onellion M, Chang Y, Niles D W, Joynt R, Margaritondo G, Stoffel N G and Tarascon J M 1987 *Phys. Rev. B* **36** 819
[34] Sternemann C, Sternemann H, Huotari S, Lehmkühler F, Tolan M and Tse J S 2008 *J. Anal. Atom. Spectrom.* **23** 807
[35] Schülke W 2007 *Electron dynamics by inelastic x–ray scattering* (Oxford University Press)
[36] Huotari S, Pylkkänen T, Verbeni R, Monaco G, and Hämäläinen 2011 *Nature Mater.* **10** 489
[37] Nagasawa H, Mourikis S and Schülke 1997 *J. Phys. Soc. Japan* **66** 3139
[38] Verbeni R, Pylkkänen T, Huotari S, Simonelli L, Vankó G, Martel K, Henriquet C and Monaco G 2009 *J. Synchrotron. Rad.* **16** 469
[39] Fister T T, Seidler G T, Wharton L, Battle A R, Ellis T B, Cross J O, Macrander A T, Elam W T, Tyson t A and Qian Q 2006 *Rev. Sci. Instrum.* **77** 063901
[40] Sternemann H, Sternemann C, Seidler G T, Fister T T, Sakko A and Tolan M 2008 *J. Synchrotron. Rad.* **15** 162
[41] Gordon R A, Seidler G T, Fister T T, Haverkort M W, Sawatzki G A, Tanaka A and Sham T K 2008 *Europhys. Lett.* **81** 26004
[42] Tse J S, Yang L, Zhang S J, Jin C Q, Sahle Ch J, Sternemann C, Nyrow A, Giordano V, Jiang J Z, Yamanaka S, Desgreniers S and Tulk C A 2011 *Phys. Rev. B* **84** 184105
[43] Ankudinov A L, Nesvizhskii A I and Rehr J J 2003 *Phys. Rev. B* **67** 115120
[44] Sternemann C, Volmer M, Soininen J A, Nagasawa H, Paulus M, Enkisch H, Schmidt G, Tolan M and Schülke W 2003 *Phys. Rev. B* **68** 035111
[45] Diamant R, Huotari S, Hämäläinen K, Sharon R, Kao C-C and Deutsch M 2006 *Radiat. Phys. Chem.* **75** 1434 and references therein.
[46] Crljen Z, Luberek J, Wendin G and Levine Z H 1993 *Phys. Rev. A* **50** 3529
[47] Cowan R D 1981 *The Theory of Atomic Structure and Spectra* (Los Alamos Series in Basic and Applied Sciences)
[48] Phaneuf R A, Kilcoyne A L D, Aryal N B, Baral K K, Esteves-Macaluso, Thomas C M, Hellhund J, Lomsadze R, Gorczyka T W, Ballance C P, Manson S T, Hasoglu M F, Schippers S, and Müller A 2013 *Phys. Rev. A* **88** 053402